Received: 29 April 2022 | Accepted: 1 July 2022

DOI: 10.1111/jth.15817

ORIGINAL ARTICLE

# Characterization of interaction between blood coagulation factor VIII and LRP1 suggests dynamic binding by alternating complex contacts

Haarin Chun[1] | James H. Kurasawa[1] | Philip Olivares[1] | Ekaterina S. Marakasova[1] | Svetlana A. Shestopal[1] | Gabriela U. Hassink[1] | Elena Karnaukhova[1] | Mary Migliorini[2] | Juliet O. Obi[3] | Ally K. Smith[3] | Patrick L. Wintrode[3] | Prasannavenkatesh Durai[4] | Keunwan Park[4] | Daniel Deredge[3] | Dudley K. Strickland[2] | Andrey G. Sarafanov[1]

[1]Center for Biologics Evaluation and Research, U.S. Food and Drug Administration, Silver Spring, Maryland, USA

[2]Center for Vascular and Inflammatory Diseases, Departments of Surgery and Physiology, University of Maryland School of Medicine, Baltimore, Maryland, USA

[3]Department of Pharmaceutical Sciences, University of Maryland School of Pharmacy, Baltimore, Maryland, USA

[4]Natural Product Informatics Research Center, Korea Institute of Science and Technology, Gangneung, Republic of Korea

**Correspondence**
Andrey G. Sarafanov, Center for Biologics Evaluation and Research, U.S. Food and Drug Administration, 10903 New Hampshire Avenue, Silver Spring, MD 20993, USA.
Email: andrey.sarafanov@fda.hhs.gov

**Present address**
James H. Kurasawa, Biologics Engineering, R&D, AstraZeneca, Gaithersburg, Maryland, USA

Ekaterina S. Marakasova, (1) Center for Devices and Radiological Health, U.S. Food and Drug Administration, Silver Spring, Maryland, USA and (2) George Mason University, School of Systems Biology, Fairfax, Virginia, USA

Gabriela U. Hassink, GSK-Rockville Center for Vaccines Research, Rockville, Maryland, USA

## Abstract

**Background:** Deficiency in blood coagulation factor VIII (FVIII) results in life-threating bleeding (hemophilia A) treated by infusions of FVIII concentrates. To improve disease treatment, FVIII has been modified to increase its plasma half-life, which requires understanding mechanisms of FVIII catabolism. An important catabolic actor is hepatic low density lipoprotein receptor-related protein 1 (LRP1), which also regulates many other clinically significant processes. Previous studies showed complexity of FVIII site for binding LRP1.

**Objectives:** To characterize binding sites between FVIII and LRP1 and suggest a model of the interaction.

**Methods:** A series of recombinant ligand-binding complement-type repeat (CR) fragments of LRP1 including mutated variants was generated in a baculovirus system and tested for FVIII interaction using surface plasmon resonance, tissue culture model, hydrogen–deuterium exchange mass spectrometry, and in silico.

**Results:** Multiple CR doublets within LRP1 clusters II and IV were identified as alternative FVIII-binding sites. These interactions follow the canonical binding mode providing major binding energy, and additional weak interactions are contributed by adjacent CR domains. A representative CR doublet was shown to have multiple contact sites on FVIII.

**Conclusions:** FVIII and LRP1 interact via formation of multiple complex contacts involving both canonical and non-canonical binding combinations. We propose that FVIII-LRP1 interaction occurs via switching such alternative binding combinations in a dynamic mode, and that this mechanism is relevant to other ligand

Manuscript handled by: Alan Mast

Final decision: Alan Mast, 01 July 2022

**Funding information**
School of Pharmacy Mass Spectrometry Center, University of Maryland Baltimore, Grant/Award Number: SOP1841-IQB2014; U.S. Department of Energy; Ministry of Oceans and Fisheries, Korea, Grant/Award Number: 20210647 (KP); U.S. FDA/CBER project 05010 (AGS); R35HL135743 (DKS)

interactions of the low-density lipoprotein receptor family members including LRP1.

**KEYWORDS**
blood coagulation, factor VIII, hemophilia A, LDL-receptor related protein-associated protein, low density lipoprotein receptor, low density lipoprotein receptor-related protein 1

## 1 | INTRODUCTION

Blood coagulation factor VIII (FVIII) is a large heterodimeric protein (~300 kDa) consisting of a heavy chain (HCh, A1-A2-B domains) and a light chain (LCh, A3-C1-C2 domains). It circulates in complex with von Willebrand factor (VWF), which stabilizes FVIII in plasma.[1,2] At coagulation sites, FVIII is site-specifically cleaved by thrombin into activated FVIII (FVIIIa) (Figure S1 in supporting information), which serves as cofactor to activated factor IX in reactions of blood clotting.[3] Congenital FVIII deficiency results in life-threatening bleeding (hemophilia A) treated by infusions of therapeutic FVIII. To reduce infusion frequency, extended plasma half-life FVIII variants are being generated,[4] and optimal designs require understanding FVIII catabolic mechanisms.

Plasma clearance of FVIII involves several receptors[5–14] with hepatic low density lipoprotein receptor-related protein 1 (LRP1) playing a major role.[7,9,15–19] In a pathway with direct FVIII–LRP1 interaction, it occurs via a small FVIII fraction (~5%) unbound to VWF and preconcentrated on cell surfaces.[20–22] In FVIII clearance, LRP1 acts in concert with the hepatic low density lipoprotein receptor (LDLR).[5] Both belong to the LDLR family of endocytic receptors[23–26] associated with many processes with clinical significance.[27–31] Other members of the LDLR family, very low density lipoprotein receptor (vLDLR) and megalin, can also interact with FVIII with unknown functional relevance.[32,33]

LRP1 is ubiquitously expressed in many tissues where it interacts with numerous ligands to regulate many processes of which pathology may cause type 2 diabetes, obesity, and Parkinson's and Alzheimer's diseases.[27,28,30,31] In circulation, LRP1 internalizes diverse structurally unrelated ligands including triglyceride-rich particles, proteases and their complexes with inhibitors, and coagulation proteins.[34,35] The ligand-binding moiety of LRP1, as well as other LDLR family members, is presented by clusters of highly homologous complement-type repeats (CR; Figure S2 in supporting information) forming autonomous domains. The domain structure is enforced by three disulfide bonds and $Ca^{2+}$ coordination via four conserved acidic residues.[16,36,37] During ligand binding, these acidic residues and a conserved aromatic residue interact with a $\varepsilon$-amino group and an aliphatic chain of a ligand's lysine (termed "critical"), respectively, while other interface residues also contribute to interaction. This mode (termed "canonical") was described for interaction of LDLR with receptor-associated protein (RAP), a folding chaperone of the receptor's family,[38] and was proposed as a common mechanism for ligand recognition by these receptors.[39,40] Based on the chaperone function and ability to interact with all receptors of LDLR family, RAP has been considered a model ligand of the family.[41–43]

**Essentials**

- Factor VIII (FVIII) is catabolized by low density lipoprotein receptor-related protein 1 (LRP1).
- Multiple LRP1 sites for binding FVIII were identified and characterized.
- Multiple FVIII sites for binding a particular LRP1 fragment were identified.
- We propose a model of FVIII–LRP1 interaction based on dynamically alternating complex contacts.

In the RAP–LRP1 interaction, a doublet of adjacent CR domains of LRP1 binds two critical lysine residues of RAP providing canonical interaction (termed "bivalent") via switching contacts dynamically.[44–46] In FVIII–LRP1 interaction, at least two charged FVIII residues were also proposed to bivalently interact with LRP1 suggesting similarity of the mechanism.[46] While multiple lysine residues on FVIII were shown to be important for binding,[47] extensive mutagenesis of lysines on FVIII did not abolish its interaction with LRP1[7,47] indicating its complexity. In LRP1, among the four clusters with 31 CR domains in total (Figure 1A and Figure S2), clusters II and IV were shown to bind the isolated FVIII LCh.[48–50] Together, these data indicate complexity of the interactive determinants on both proteins.

Here, we aimed to characterize the minimal bivalent binding sites of LRP1 for FVIII, verify their relevance to the canonical binding mode, and elucidate a relationship between the relative simplicity of the bivalent mechanism and complexity of the interactive determinants on both proteins. Our experimental approaches include expressing LRP1 fragments and determining their interactions with FVIII in purified systems, tissue culture, and in silico.

## 2 | MATERIALS AND METHODS

### 2.1 | Proteins

Recombinant full-length FVIII products A and B, and a B domain-deleted FVIII (BDD–FVIII) product C were obtained from ASD Healthcare and National Institute of Health Pharmacy. These products were used interchangeably as a source of FVIII with no difference in results: product A was used in most experiments, while products B (Figure S6D in supporting information) and C (Table S1 and Figure S3 in supporting information) were used in experiments in indicated figures. Plasma-derived FVIII (pdFVIII) was prepared

as described.[51] A B domain–truncated FVIII bearing 21 amino acids of the B domain[52] was kindly provided by Novo Nordisk and used in hydrogen–deuterium exchange mass spectrometry (HDX-MS) experiment. Recombinant FVIII LCh and scFv iKM33 were prepared as described.[53] LRP1 was isolated as described,[54] and its CR fragments were generated using DNA synthesis (GenScript) and Bac-to-Bac Baculovirus Expression System (Thermo Fisher Scientific) as described.[51] CR fragments used in experiments shown in Figures 2A–D, 4C and 5 and Figure S4A in supporting information were generated using RAP co-expression.[45] RAP was purchased from R&D Systems. Protein concentrations were determined by measuring the UV absorbance at 280 nm based on extinction coefficients calculated using ProtParam (Expasy).

## 2.2 | Antibodies, cell lines, reagents, and polyacrylamide gel electrophoresis

Anti-LRP1 (1:5000) and LDLR antibodies (1:2000) were purchased from Abcam. Secondary antibodies (IRDye 680RD Goat anti-Rabbit and IRDye 800CW Donkey anti-Mouse, 1:10 000) and anti-β-actin antibody (1:5000) were purchased from LI-COR

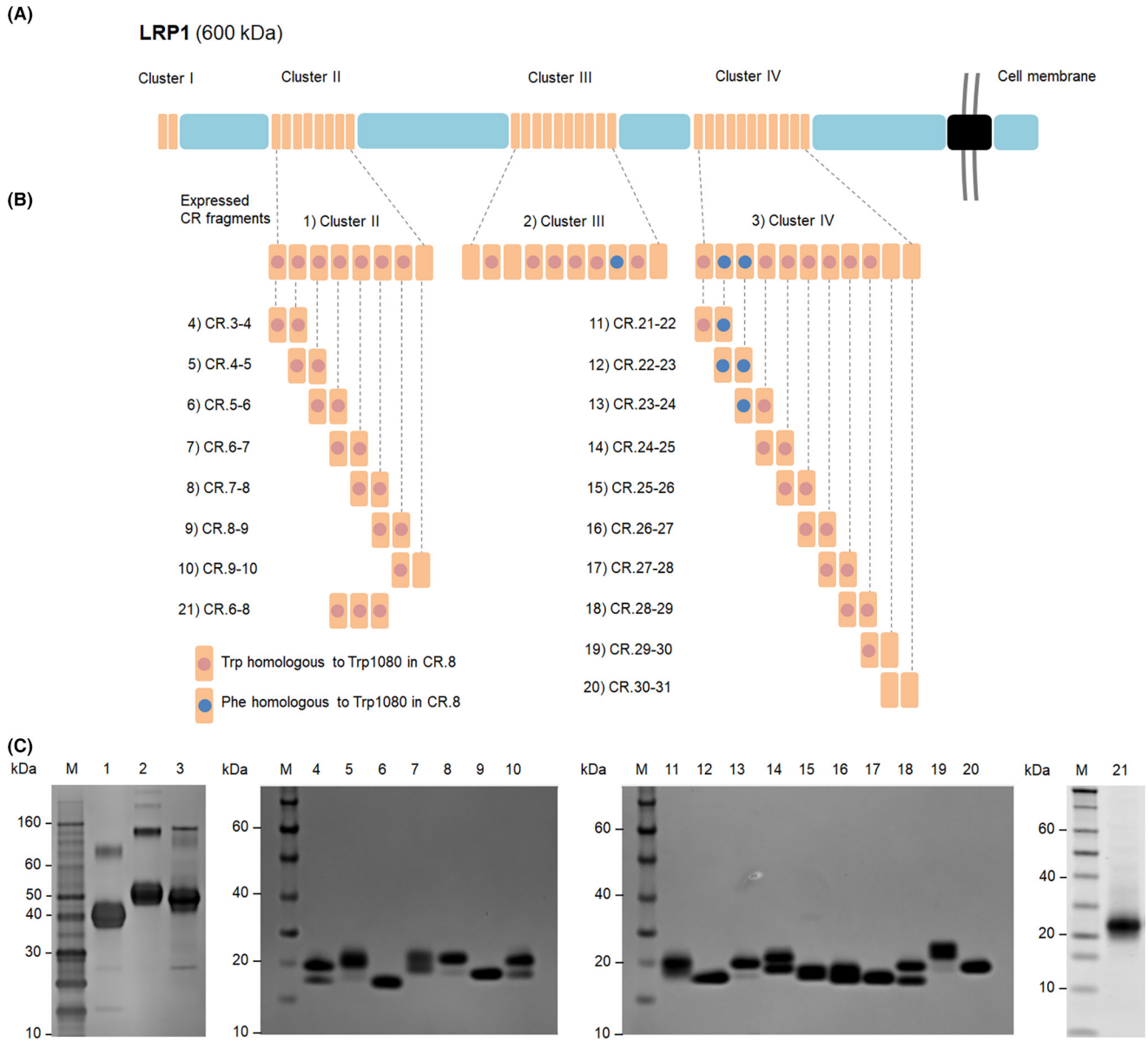


FIGURE 1 The complement-type repeat (CR) domain structure of lipoprotein receptor-related protein 1 (LRP1) and expressed CR fragments. (A) CR domain structure of LRP1. (B) Expressed CR fragments of LRP1: individual CR domains are depicted by rectangles, where the conserved aromatic residues homologous to W1080 in CR.8 (position 1 in Figure S2) are indicated by circles (pink for tryptophan and blue for phenylalanine). (C) Analysis of purified clusters II–IV and CR fragments overlapping clusters II and IV by sodium dodecyl sulfate polyacrylamide gel electrophoresis (non-reducing condition) gels stained with Coomassie Brilliant Blue. Line numbering corresponds to the numbering of the protein samples; M, molecular weight markers.

Biosciences. For flow cytometry, polyclonal anti-FVIII antibody (Enzyme Research Laboratories) was conjugated to Alexa Fluor 647 dye (Thermo Fisher Scientific). HepG2, Hep3B, and SK-HEP1 cells were purchased from American Type Culture Collection (ATCC), and Huh-7 cells were purchased from Sekisui XenoTech. Cells were cultured according to manufacturer's instructions. Cells were transfected with siRNAs purchased from Dharmacon using DharmaFECT. Protein lysates (40 μg) were prepared as described[55] from HepG2, Hep3B, Huh-7, and SK-HEP1 cells and separated on a 4%–12% NuPAGE Bis-Tris Protein Gel (Thermo Fisher Scientific). Chameleon Duo Pre-Stained Protein Ladder (LI-COR) was used as control. For quantification of LRP1 and LDLR expression, immunoblot band intensities were determined by Image Studio Lite (LI-COR Biosciences).[56]

## 2.3 | Circular dichroism

Far-UV circular dichroism (CD) spectra were measured using a Jasco J-815 Spectropolarimeter equipped with a PTC 423S/15 Peltier temperature controller (Jasco) at 25 ± 0.2°C. The protein concentration in the samples was adjusted to 30 μM in HBS buffer (10 mM HEPES pH 7.4, 150 mM NaCl) containing 5 mM $CaCl_2$. Ethylenediaminetetraacetic acid (EDTA) titration of samples was conducted as described.[45,57] Measurements were conducted between 180 and 260 nm using a 0.5-mm path length quartz cuvette at a scan speed of 20 nm/min, bandwidth of 1.0 nm, and resolution of 0.2 nm, and accumulated in triplicate.

## 2.4 | Surface plasmon resonance

LRP1 and its fragments were immobilized on CM5 sensor chips using an amine coupling kit (Cytiva) at indicated level (RU). Binding assays were performed in HBS-P buffer (Cytiva) supplemented with 5 mM $CaCl_2$ (HBS-P/Ca) using a Biacore 3000 or T200 instrument (Cytiva). Association and dissociation of analytes were recorded at 30 μl/min for 2 and 3 min, respectively. Sensor chip regeneration was conducted with 0.1 M $H_3PO_4$ (50 μl/min). For the competitive binding assay shown in Figure 5A, CR.7–8 was biotinylated using EZ-Link Sulfo-NHS-Biotin (Thermo Fisher Scientific) and purified by Zeba Spin Desalting Columns, 7 K MWCO (Thermo Fisher Scientific). Biotinylated CR.7–8 (50 nM) was captured by pre-immobilized streptavidin-oligonucleotide on a CAP sensor chip (Cytiva). FVIII (25 nM), in presence and absence of cluster II fragments (125 nM) in HBS-P/Ca buffer, was injected over the chip. Binding signals were recorded upon increasing FVIII concentrations for four repeat sets. To assess the FVIII affinities upon the LRP1 sites mapping, a 1:1 Langmuir model fit was applied on the surface plasmon resonance (SPR) signals using BIAevaluation v4.1.1 software (Cytiva). For fitting other binding data, the steady-state affinity and bivalent analyte models were used with T200 v3.2 software (Cytiva).

## 2.5 | Cell-based FVIII internalization assay

Seventy percent of confluent Huh-7 cells cultured in 6-well tissue culture plates coated with poly-D-lysine (Sigma) in Dulbecco's modified Eagle's medium (DMEM) with low glucose and 10% fetal bovine serum were exposed to serum-free DMEM containing 10 mM HEPES, 5 mM $CaCl_2$, and 150 mM NaCl for 2 h. Media was changed to fresh pre-warmed serum-free DMEM containing 1% bovine serum albumin (BSA), 10 mM HEPES, 5 mM $CaCl_2$, 150 mM NaCl, and then FVIII, LRP1 fragments, iKM33, or RAP were added as indicated. After 1 h incubation at 37°C, cells were washed with PBS and detached by treating with Accutase. Cells were collected by centrifuging at 100 ***g*** at 4°C for 6 min, incubated with phosphate-buffered saline (PBS) containing LIVE/DEAD fixable Aqua dead cell stain for 405 nm excitation (Thermo Fisher Scientific) at 4°C for 30 min, washed with PBS, and treated with 4% paraformaldehyde (Thermo Fisher Scientific) for 15 min. Washed cells were treated with the staining solution (0.1% saponin and 1% BSA) for 20 min followed by incubation with the labeled FVIII antibody (1:100) at room temperature for 20 min. Collected cells were sequentially washed with the staining solution and PBS, resuspended in PBS, and analyzed using a FACS Canto II Flow Cytometer (BD Biosciences Systems). Internalized FVIII levels were quantified after subtracting non-treated sample (5000–10 000 cells per sample) by analyzing mean fluorescence intensities in viable cells.

## 2.6 | Hydrogen deuterium exchange-mass spectrometry

Sequence coverage determination and HDX-MS experiments were performed as described[58,59] with the following conditions. FVIII and CR.7–8 samples were buffer exchanged into 20 mM imidazole pH 7.3, 10 mM $CaCl_2$, and 500 mM NaCl. For the FVIII sequence coverage map, 0.5 μl of 25 μM FVIII was added to 39.5 μl of ice-cold quench (50 mM glycine, pH 2.5, and 6 M guanidine-HCl) before diluting in 100 mM glycine. Two hundred μl of the solution was injected into a Waters HDX system (Waters) with in-line Enzymate BEH Pepsin Column (Waters). HDX-MS reactions of FVIII and FVIII/CR.7–8 complex were performed in triplicate at 25°C for 10 s, 1, 10, and 60 min using a LEAP autosampler as follows: reactions were initiated by combining 2 μl of 20 μM protein with 18 μl of $^2H_2O$ buffer (pD 7.3, 20 mM imidazole, 10 mM $CaCl_2$, and 111 mM NaCl) resulting in a 150 mM final NaCl concentration favoring FVIII/CR.7–8 complex formation. The reactions were quenched by adding 50 μl of ice-cold quench (50 mM glycine, 6 M guanidine, and 100 mM tris [2-carboxyethyl]phosphine). The solution was then diluted in 180 μl of 100 mM glycine and injected after 2 min incubation.

## 2.7 | Structural modeling and docking simulation

The structural model for CR.7–8 was generated by multi-template homology modeling with MODELER[60] with template structures for CR.7 (PDB ID 1J8E) and CR.8 (PDB ID 5B4X). Based on the previous

findings[38,44] and our experimental data, it was assumed that both CR.7 and CR.8 interact with FVIII lysines through the conserved calcium-coordinating acidic residues (Figure S2) on CR.7–8. Thus, the two aspartic acid residues and one tryptophan in the CR calcium binding pocket was used to define distance-based constraints during the subsequent docking simulations to FVIII (PDB ID 6MF2). The ideal lysine interaction distances to W144, D147, and D151 (NZ atom in lysine and CG atom in tryptophan or aspartic acid) were set to 4.2, 3.4, and 3.5 Å, respectively, by referring to the X-ray crystal structure of RAP complexed with LDLR (PDB ID 2FCW).[38] For the 10 lysines found in FVIII LCh by HDX-MS, docking simulation was performed by Rosetta FastRelax[61] with constraints for 250 times, and the model with the lowest binding energy was finally selected.

### 2.8 | Statistics

Statistical significance was determined using one-way or two-way analysis of variance followed by Tukey's post hoc test in GraphPad Prism, v7.04 (GraphPad Software). All data are presented as mean ± standard deviation (SD), and $p < .05$ were considered statistically significant.

## 3 | RESULTS

### 3.1 | Testing FVIII interactions with LRP1 and its clusters II–IV

To examine the structure–function relationship of FVIII-binding regions of LRP1, we compared FVIII binding to LRP1 and its recombinant clusters II–IV (Figure 1A,B) by SPR. Here and further, we used LRP1 fragments generated in insect cells proven to produce functional CR fragments of the LDLR family.[45,51,57] FVIII bound in similar fashion to LRP1 and its clusters II and IV (Figure 2A–D), consistent with previous studies.[46,48,50] The assessed affinities were comparable ($K_D$s ~ 20 nM, Table 1) indicating functional equivalency of these interactions.

Specificity of interactions was tested using iKM33, a single-chain variable antibody fragment (scFv) recognizing FVIII C1 domain.[53,62] In a dose-dependent manner, iKM33 strongly inhibited FVIII binding to the tested proteins (Figure S4A) indicating an involvement of FVIII C1 domain or its proximal regions in these interactions.

### 3.2 | Identification of LRP1 CR doublets binding FVIII

Previous studies indicated that a minimal binding site of LRP1 for FVIII is formed by a pair of adjacent CR domains similarly to RAP binding.[51,57] To identify those within clusters II and IV, we generated a series of CR doublets overlapping both clusters (Figure 1B). By PAGE, some proteins showed two bands (Figure 1C) attributed to differential glycosylation based on previous studies.[50,51,57] By SPR, CRs 6–7, 7–8, 24–25, and 28–29 showed the strongest binding (Figure 2E,F and Figure S3) with $K_D$s of 40–70 nM to various FVIII species (Table S1). Specificity of the interactions was tested using iKM33 as a competitor, where its 5-fold molar excess suppressed all interactions (Figure S4B,C). This indicates an importance of FVIII C1 and/or its adjacent domains for the binding.

To ensure proper folding of the CR doublets, secondary structures of selected "weak binders" (CR.3–4 and 4–5) and "strong binders" (CR.6–7 and 7–8) were assessed by far-UV CD as described.[45] All proteins exhibited similar spectra, and their titration with EDTA to remove bound $Ca^{2+}$ important for the folding showed comparable reduction of the major negative extremum at ~200 nm (Figure S5 in supporting information). This indicates similar folding of all CR doublets and supports validity of the SPR results.

### 3.3 | Mutational analysis of FVIII interactions with LRP1 fragments

Previous studies showed the importance of the conserved aromatic residues in the LDLR family for ligand interactions.[38–40,57] To verify this for FVIII and LRP1, we generated a series of LRP1 fragments carrying substitutions of the conserved tryptophan (Figure S2) to serine, which does not affect CR domain folding but disrupts the canonical binding.[51,57,63] The mutations were introduced to strong and moderate FVIII-binding CRs within the clusters (CRs 5–9 in cluster II, and CRs 24–29 in cluster IV) and their doublets CR.7–8 and CR.28–29, but not to other CRs showed low FVIII binding (Table S1) or lacking the conserved tryptophan (Figure S2).

By SPR, the mutant proteins exhibited reduced binding to both RAP and FVIII (Figure 3). These results indicate the significance of the conserved tryptophan residues similar to that previously shown for RAP and other ligands of the LDLR family members[38–40,63] and support relevance of the canonical binding mode to FVIII interactions. Notably, the reduced binding of mutant proteins was more pronounced for RAP compared to FVIII, and for CR doublets compared to the clusters. This is in line with previous studies showing that RAP binding is predominantly dependent on the canonical interactions of its critical lysine residues,[45,64] whereas FVIII binding involves additional determinants within both mutated and non-mutated CR domains, mitigating the mutational effect. The results also show that non-mutated CR domains within the clusters may contribute to FVIII binding (Figure 3F,H) consistent with the ability of these CRs within isolated CR doublets to weakly bind FVIII (Figure 2).

### 3.4 | Development of LRP1-mediated FVIII internalization tissue culture model

To confirm the role of CR doublets in FVIII-LRP1 interaction, we developed a tissue culture model of LRP1-mediated FVIII internalization. For cell line selection, we compared LRP1 and LDLR expression levels in human hepatic cell lines HepG2, Hep3B, Huh-7, and SK-HEP1 as both receptors are expressed in liver where they contribute to FVIII clearance and Huh-7 showed the highest abundance of LRP1 over LDLR (Figure S6A). Then, time- and

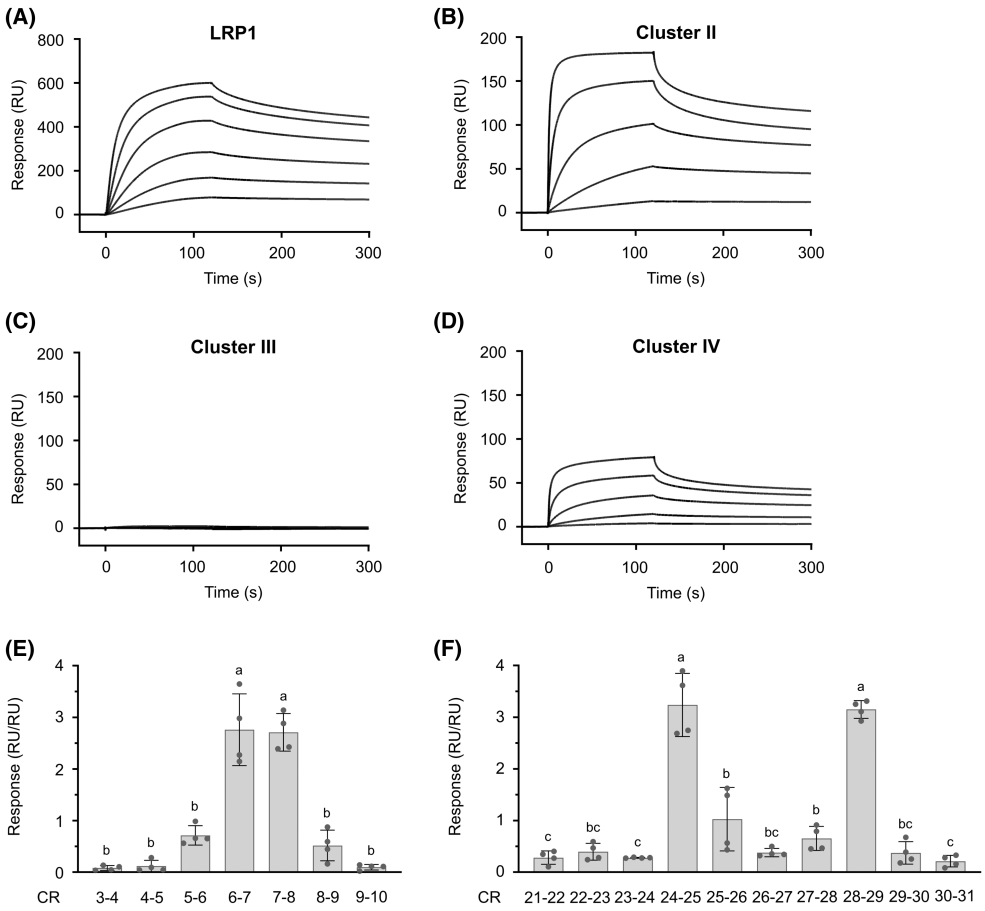


FIGURE 2 Testing factor VIII (FVIII) interactions with lipoprotein receptor-related protein 1 (LRP1) fragments by surface plasmon resonance (SPR). LRP1 (A) and its clusters II, III, and IV (B–D) were immobilized at ~250 RU and tested for binding with FVIII (2.5, 5, 10, 20, 40, and 80 nM for LRP1, and 0.5, 1.9, 7.5, 30, and 120 nM for LRP1 clusters) using a Biacore T200 instrument. The representative graphs of the three independent experiments are shown. RU, resonance units. (E,F) Binding FVIII to complement-type repeat (CR) doublets of LRP1 clusters II (E) and IV (F). The CR doublets were immobilized on a sensor chip at ~1000 RU and tested for binding with FVIII (125 and 200 nM) using a Biacore 3000 instrument. The maximum responses during 3 min of association were normalized per RU of the CR doublet immobilization level (RU/RU) multiplied by 10 for convenience of data visualization and further normalized to the average of the four independent experimental data to adjust scales. The experiments were conducted with 2-fold serial dilutions of each ligand, while the bars presented are for a selected concentration of each ligand. Data are presented as mean ± standard deviation from four independent SPR experiments using two independently expressed and purified sets of CR doublets. Values with one different letter are significantly different from each other ($p < .05$; one-way analysis of variance, Tukey's post hoc test).

temperature-dependent FVIII internalization by the cells were measured using polyclonal anti-FVIII antibodies and flow cytometry (Figure S6B,C), and the highest level of internalized FVIII was observed in Huh-7 cells (Figure S6D).

Relative contributions of LRP1 and LDLR for FVIII internalization in Huh-7 cells were tested using small interfering RNA (siRNA). Compared to cells treated with non-targeting siRNA, depletion of either LRP1 or LDLR resulted in ~70% or ~30% reduction in FVIII internalization, respectively, whereas the depletion of both receptors did not further decrease FVIII internalization compared to LRP1 depletion only. In control experiments, additional treatment with either RAP or iKM33 showed reduced FVIII internalization comparable to the LRP1-depleted condition (Figure 4A,B). Altogether, the results show that LRP1 is the major endocytic receptor of FVIII under the tested conditions.

### 3.5 | Testing LRP1-mediated FVIII internalization in the presence of LRP1 fragments

We next ascertained significance of CR fragments for FVIII interaction using our tissue culture model. Various molar ratios of cluster II, III, or IV were pre-incubated with FVIII and treated to Huh-7 cells followed by internalized FVIII quantitation. Clusters II and IV inhibited FVIII internalization dose dependently (Figure S7 in supporting information), and at 10-fold molar excess, lowered internalization by ~40% and ~30%, respectively, in contrast to cluster III showing no significant effect (Figure 4C). The results are consistent with SPR data (Figure 2B–D) and indicate the overlapping FVIII binding sites within clusters II and IV, and their independent role within LRP1 in FVIII internalization.

In similar testing conditions with CR doublets overlapping clusters II and IV, CRs 7–8, 24–25, and 28–29 suppressed FVIII internalization

**TABLE 1** Equilibrium binding constants for FVIII interactions with LRP1 and its recombinant fragments

| LRP1/fragment | $K_D$ (nM) |
|---|---|
| LRP1 | 22.8 ± 5.2 |
| Cluster II | 11.3 ± 0.8 |
| Cluster III | NBD |
| Cluster IV | 19.6 ± 3.3 |
| CR.6–8 | 28.4 ± 8.9 |
| CR.6–7 | 65.2 ± 12.9 |
| CR.7–8 | 81.5 ± 26.3 |
| CR.7 | NBD |

*Note*: Binding experiments were performed using SPR. The $K_D$ values were calculated by fitting the data to a steady-state affinity model. Values are average ± SD from three different experiments.

Abbreviations: CR, complement-type repeat; FVIII, factor VIII; LRP1, lipoprotein receptor-related protein 1; NBD, no binding detected; SD, standard deviation; SPR, surface plasmon resonance.

(Figure 4D,E), consistent with their strong FVIII binding in SPR (Figure 2E,F). CR.22–23 (a weak FVIII binder) also inhibited FVIII internalization, while CR.6–7 (a strong FVIII binder) did not affect FVIII internalization. Notably, as LRP1 accounts for ~70% of FVIII uptake in Huh-7 cells, 20%–25% reduction in the FVIII internalization corresponds to 30%–36% decrease of LRP1-mediated internalization.

We next verified whether the CR fragments compete for FVIII binding with endogenous LRP1, but not other cellular entities. CR.6–8 triplet comprised of strong binders CRs 6–7 and 7–8, and its (CR.6–8) tripple mutant (W→S) were tested with FVIII in cultures pretreated with respective siRNAs. CR.6–8 markedly inhibited internalization of FVIII by cells pretreated with non-targeting or LDLR-targeting siRNA, while CR.6–8 mutant exhibited lower suppression; no further effects were observed when LRP1 was depleted (Figure S8 in supporting information). This supports that inhibition of FVIII internalization by CR fragments depends on competition with cellular LRP1 for FVIII binding. Taken together, these results further support that CRs 7–8, 24–25, and 28–29 are major LRP1 sites for FVIII binding.

## 3.6 | Testing avidity effects of CR domains on interactions with FVIII

Previous studies to assess affinity of FVIII and LRP1 determined a $K_D$ within 18–116 nM.[7,9,47,49] We assessed this value as ~23 nM, which was comparable to isolated clusters II and IV (Table 1), whereas the strong binding CR doublets showed lower affinities (Table 1 and Table S1). To investigate whether the number of CR domains affects FVIII binding, we assessed FVIII affinity for a series of cluster II fragments: CR.7 singlet, CR doublets 6–7 and 7–8, CR triplet 6–8, and CR octet 3–10 (the full-length cluster II). Similar to clusters II–IV, these fragments were generated with RAP co-expression to ensure protein folding.[45]

By SPR, FVIII did not bind CR.7, in line with previous reports showing no or poor interaction between a CR singlet and RAP.[44,45] Other CR fragments showed a direct relationship between the fragment length and FVIII binding affinity, based on consecutive moderate decrease of the $K_D$ values upon the increase of the domains number (Table 1 and Figure S9 in supporting information).

To verify the additive (avidity) effects of CR domains, we tested the same CR fragments as competitors of FVIII interactions. CR.6–7 had no effect on FVIII binding to immobilized CR.7–8, implying that FVIII sites for binding these doublets are distantly located. Upon increasing the number of domains, other CR fragments led to progressive inhibition of binding with the strongest effect being of cluster II (Figure 5A). Similar effects of the fragments on FVIII internalization were observed in the tissue culture model (Figure 5B). Collectively, the results demonstrate that during FVIII interaction with cluster II, a CR doublet predominantly contributes to the binding energy with an additional input of other CR domains.

## 3.7 | Identification of CR.7–8 binding sites on FVIII by HDX-MS

To characterize FVIII-binding sites for a minimal binding unit of LRP1, HDX-MS was employed to analyze the complex of CR.7–8 and a B domain-truncated FVIII, which is less heterogenous than full-length FVIII while functionally equivalent to it. The analysis of FVIII in presence and absence of CR.7–8 detected a total of 264 peptides covering 78% of FVIII primary sequence. In presence of CR.7–8, overlapping peptides encompassing FVIII residues 19–27, 185–198, 222–225, 369–388, 404–410, 442–445, 487–497, 649–663, 1689–1700, 1705–1718, 1743–1752, 2034–2050, 2088–2096, 2109–2113, 2130–2134, 2146–2150, 2210–2228, 2236–2251, 2269–2274, and 2284–2294 displayed decreased deuterium uptake, indicating that these regions are protected or changed conformational dynamics (Figure 6A). When mapped onto the FVIII crystal structure, the non-contiguous nature of protected regions revealed multiple areas located throughout the molecule, prevalently on the LCh (Figure 6B). These areas include surface-exposed lysine residues, of which locations were highly comparable to those previously observed in FVIII complex with cluster II by HDX-MS.[47] This suggests that within LRP1, CR.7–8 interacts with multiple regions on FVIII that is similar to the cluster II interaction.

## 3.8 | Modeling interactions between FVIII and CR.7–8 in silico

To assess details of FVIII-CR.7–8 interaction, structural modeling was performed by docking CR.7–8 to lysine residues located on the surface of LCh identified by HDX-MS (Figure 7A), which resulted in selection of 90 docking pairs. Upon applying limitation criteria such as a binding energy (ΔΔG) threshold and the distance-based constraints between the acidic pockets of CR domains and FVIII lysines, 10 of the lowest binding energy docking models were selected as representative (Figure 7B) and superimposed (Figure S10 in supporting information). One of these models showing CR.7–8 docking to FVIII K1694 (A3

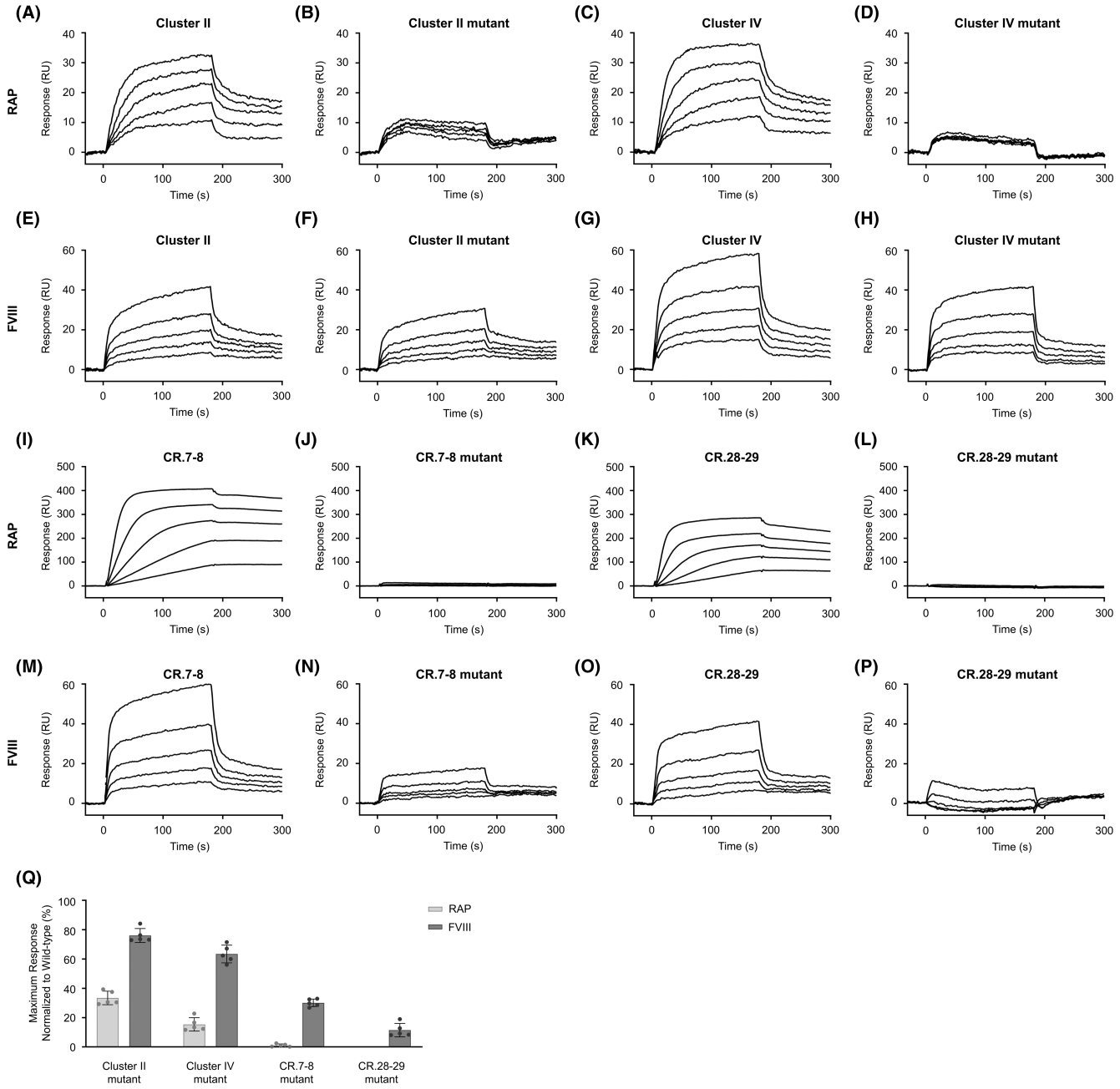


**FIGURE 3** Binding receptor-associated protein (RAP) and factor VIII (FVIII) to mutated lipoprotein receptor-related protein 1 (LRP1) clusters II and IV, and CR.7–8 and CR.28–29. In surface plasmon resonance, indicated wild-type and mutant LRP1 fragments were immobilized at ~2000 resonance unit (RU) for clusters or ~1000 RU for complement-type repeat (CR doublets, and tested for binding with RAP (0.625–10 nM; A–D and I–L) and FVIII (25–400 nM; E–H and M–P) using 2-fold serial dilutions for each ligand) and a Biacore 3000 instrument. For mutated fragments, the conserved tryptophan residues corresponding to W1080 in CR.8 (position 1 in Figure S2) were substituted to serine residues in CR.5–9 within cluster II (CR.3–10), CR.24–29 within cluster IV (CR.21–31), and in each CR domain within CR.7–8 and CR.28–29 doublets. (Q) The bars represent the maximum responses of indicated mutants at 3 min of association normalized to responses of corresponding wild-type fragments with each concentration of RAP or FVIII shown in panels (A–P).

domain) and K2092 (C1 domain) (Figure 7C) revealed: (i) electrostatic interactions between both lysines and the conserved aspartic acid residues of the CR doublet, and (ii) hydrophobic interactions between these lysines and the conserved W1032 (CR.7) and W1080 (CR.8) of the doublet, similar to that found for RAP–LDLR interaction.[38] The diverse low-energy docking combinations found here suggest that multiple FVIII sites bind CR.7–8 during the LRP1 interaction.

## 4 | DISCUSSION

The importance of LRP1 as the major FVIII clearance receptor has been well recognized, but the molecular details of this interaction have not been fully understood. In this study, we characterized FVIII binding sites of LRP1, demonstrated their multiplicity, and showed relevance of FVIII–LRP1 interaction to the canonical mode

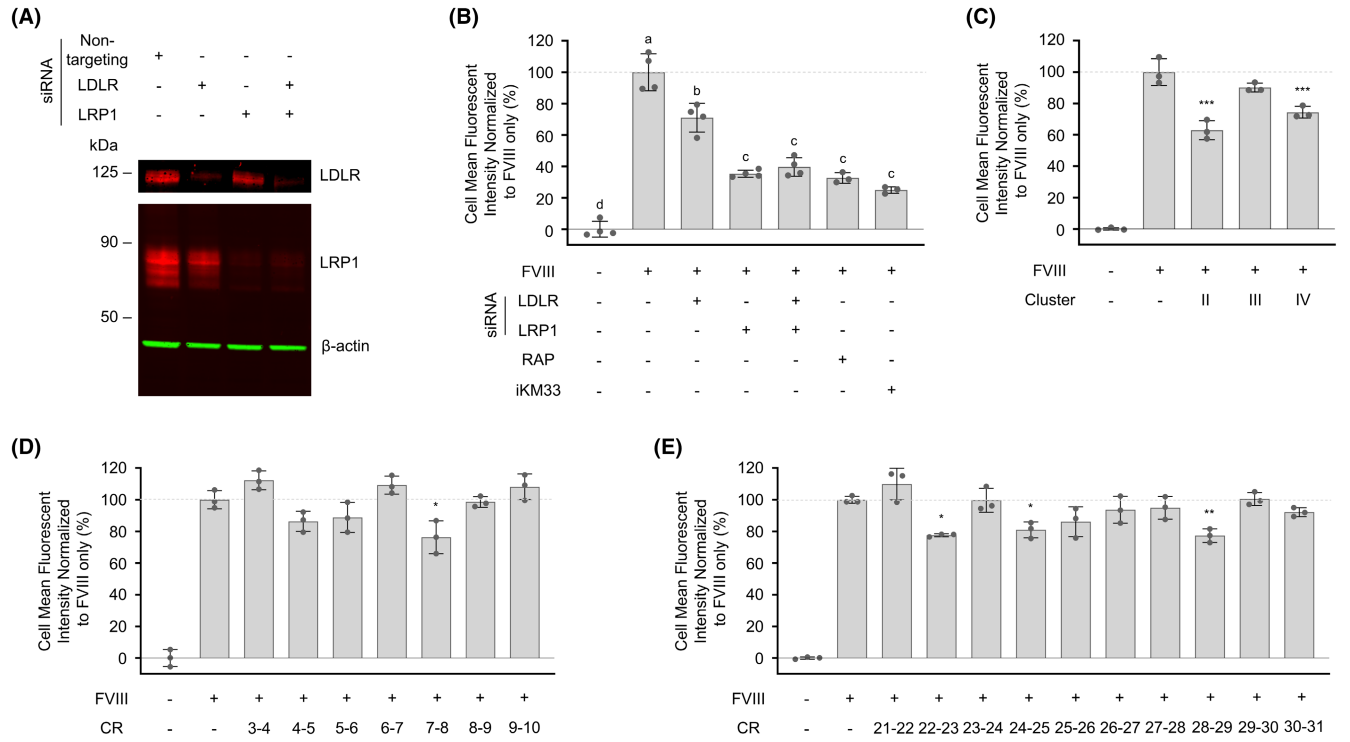


**FIGURE 4** Testing lipoprotein receptor-related protein 1 (LRP1)-mediated factor VIII (FVIII) internalization in tissue culture. In control experiments (A,B), Huh-7 cells grown in 6-well plates were incubated for 3 days with 50 nM of non-targeting siRNA or siRNA targeting LRP1 or low density lipoprotein receptor expression. Then, the cells were analyzed for receptor expression by western blotting with respective antibodies (A) or incubated with FVIII (25 nM) for 1 h at 37°C in the presence and absence of receptor-associated protein (RAP, 125 nM) or iKM33 (125 nM; B). Internalized FVIII was detected using an Alexa Fluor-647 labeled polyclonal anti-FVIII antibody and quantified by flow cytometry. The data were normalized to the amount of internalized FVIII in the cells treated with non-targeting siRNA and presented as mean ± standard deviation (SD; $n = 3–4$). Values with one different letter are significantly different from each other ($p < .05$). ***$p < .001$. Statistics: one-way analysis of variance (ANOVA), Tukey's post hoc test. C–E, Effects of LRP1 clusters II–IV and their overlapping complement-type repeat (CR) doublets on FVIII internalization in tissue culture. Huh-7 cells were incubated for 1 h with media containing FVIII (25 nM) in the presence and absence of 250 nM of cluster II, III, or IV (C), or indicated CR doublet of cluster II (D) and IV (E). The amounts of internalized FVIII were determined using flow cytometry, and the data were normalized to the amount of internalized FVIII in the absence of LRP1 fragments. Error bars indicate average ± SD of 3–4 independent experiments. Statistics: **$p < .01$; *$p < .05$, one-way ANOVA, Tukey's post hoc test.

of ligands recognition by the LDLR family receptors. Meanwhile, the complexity of interaction and relative simplicity of the canonical mechanism requires explanation.

To summarize, we showed that clusters II and IV represent independent units of LRP1 for binding FVIII, of which the major interactive sites involve the C1 and/or surrounding domains due to iKM33 interference (steric hindrance) with respective interactions. Our results indicate a major role of cluster II based on its higher affinity to FVIII and stronger inhibition of FVIII internalization in tissue culture. Notably, due to the more distant location of cluster II from the transmembrane region of LRP1 and flexibility of the molecule, cluster II has a higher capacity to spatially probe pre-concentrated FVIII on cell membranes[20] and heparan sulfate proteoglycans.[21] However, our results are in contrast to data of Young et al.,[46] who showed that cluster IV represents the major FVIII binding site, possibly due to difference in experimental conditions, in particular using recombinant protein expression ensured the protein folding by co-expressing RAP in our study.

In each cluster, we identified a series of minimal FVIII-binding sites, of which the most prominent were CRs 7–8, 24–25, and 28–29, showed strong binding to FVIII by SPR and inhibition of FVIII internalization in tissue culture. We also observed that: (i) a strong FVIII binder CR.6–7 did not affect FVIII internalization, consistent with possibly distant location of its binding site from others on FVIII (Figure S11 in supporting information), and (ii) a weak FVIII binder CR.22–23 showed strong inhibition of FVIII internalization, consistent with possible steric hindrance of its FVIII-binding site upon immobilization on solid phase, as described for relatively small ligands.[65] Thus, the doublets 6–7 and 22–23 presumably also serve as LRP1 binding sites for FVIII. Our mapping results are partially consistent with data of Meijer et al.,[50] who assessed cluster II and IV sites for binding isolated LCh using CR triplets and found ~100-fold lower affinities.

The major contribution of the canonical (bivalent) binding mode to FVIII–LRP1 interaction found by our mutational and in silico analyses agrees with the previous data showed the importance of FVIII lysine residues.[46,47] Indeed, substituting the conserved tryptophan residue in selected CR fragments resulted in reduction of their interactions with both FVIII and RAP (Figure 3), in line with

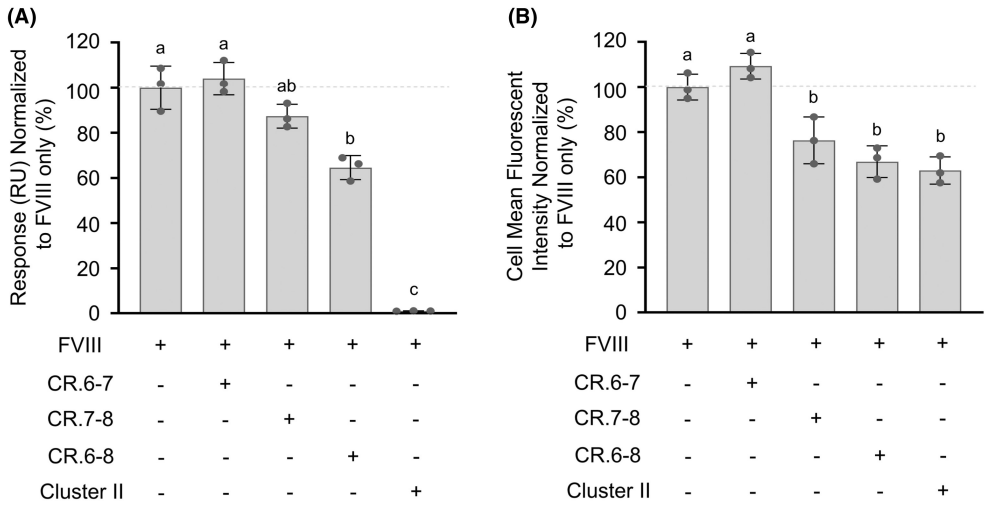


**FIGURE 5** Additive effects of complement-type repeat (CR) domains of cluster II on binding with factor VIII (FVIII). (A) In surface plasmon resonance, FVIII (25 nM) was injected over a sensor chip with captured biotinylated CR.7–8 (50 nM, pre-injected onto the chip with pre-immobilized streptavidin-oligonucleotide) in the presence and absence of CR fragments (3.9–125 nM, 2-fold dilution). Each bar height corresponds to the maximum response during 3 min of association normalized to the control FVIII injection without any cluster II fragment. Data are presented as mean ± standard deviation (SD; $n = 3$) and means marked with different letter superscripts are significantly different at $p = .05$ (one-way analysis of variance [ANOVA], Tukey's post hoc test). B, FVIII (25 nM) was incubated with Huh-7 cells in the presence and absence of CR fragments (250 nM) for 1 h at 37°C, and the amount of internalized FVIII was quantified using flow cytometry. The data were normalized to the amount of internalized FVIII only in cells and presented as mean ± SD ($n = 3$). Means that do not share a letter are significantly different each other ($p < .05$). Statistics: one-way ANOVA, Tukey's post hoc test.

importance of this residue for RAP–LDLR interaction.[38] However, in contrast to RAP–LRP1 interaction based on the canonical (bivalent) binding a CR doublet,[45] FVIII–LRP1 interaction involves additional CR domains via a non-canonical mechanism. Indeed, addition of a third canonical valency by urokinase-type plasminogen activator (uPA) to the bivalent complex of plasminogen activator inhibitor 1 (PAI-1)–LRP1 dramatically elevates the receptor's affinity (~100-fold decrease in $K_D$).[66] Respectively, removal of a canonical valency from the bivalent complexes of RAP-D3-LRP1 or RAP-CR doublet by mutating the critical lysines of RAP led to comparable shift in $K_D$ (10- to 100-fold increase).[45,67] In contrast, in our study, addition of a third and further CR domains to the model CR doublets resulted in only moderate increase in binding affinity (~2.5-fold decrease of $K_D$, Table 1). We propose that the additional interactions occur via non-canonical weak predominantly electrostatic contacts between the negatively charged acidic residues coordinating $Ca^{2+}$ in CRs and positively charged residues on FVIII. This hypothesis is supported by results of van den Biggelaar et al.[47] showed that mutations of FVIII lysine residues into oppositely charged glutamic acid resulted in more pronounced decrease in LRP1 binding compared to mutations into arginine unable to engage in the canonical interaction.[68] Thus, most CR domains of a cluster (II or IV) form a real-time interactive site where they provide both canonical bivalent and non-canonical interactions. Similarly to that, the interactive site of LRP1 for the uPA–PAI-1 complex was previously suggested to involve 4–6 CR domains with dominant contribution of a CR doublet.[63]

Our results indicate that during such interaction, a particular CR domain may: (i) form a pair with either of adjacent CR domains for alternative canonical bivalent interaction with FVIII, (ii) switch this role to the non-canonical (electrostatic) interaction, and (iii) bind multiple (alternative) sites on FVIII. Indeed, in cluster II, CR.7 could form the canonical pair with either of adjacent CR 6 or 8 as was within respective isolated CR doublets, whereas one of these domains within the isolated CR.6–8 triplet switched its role to the non-canonical interaction. Importantly, in the canonical interactions, CRs 6–7 and 7–8 were found to have distantly located binding sites on FVIII (Figure 5A) showing the doublets' alternative interactions with FVIII and multiplicity of CR.7 binding sites on FVIII, also supported by HDX-MS analysis. Notably, locations of the CR.7–8 interactive regions on FVIII by HDX-MS are highly similar to those of cluster II also found by HDX-MS,[47] indicating that CR.7–8 is the major FVIII-binding site of the cluster. In turn, in cluster IV, the strong FVIII binders CRs 24–25 and 28–29 (and likely 22–23) may form also alternative canonical (bivalent) binding combinations during the interaction.

In the resulting model of FVIII–LRP1 interaction, FVIII is initially recognized by an extended string of CR domains via multiple weak electrostatic interactions. This facilitates subsequent docking of a pair of CR domains of cluster II or IV to the C1 and/or its surrounding domains in the canonical (bivalent) binding mode that accounts for substantial binding energy. Then, the contacts are reestablished in a dynamic mode, thus multiple CR domains of the cluster engage or disengage in the interaction where they may change their role from the canonical to non-canonical interactions extending to multiple FVIII sites. The resulting complex is formed by alternatively switching such contacts in dynamic equilibrium (Figure 7D). Considering an average distance of 25 Å between the acidic pockets of adjacent CR domains[28] and flexibility of interdomain linkers facilitating domain

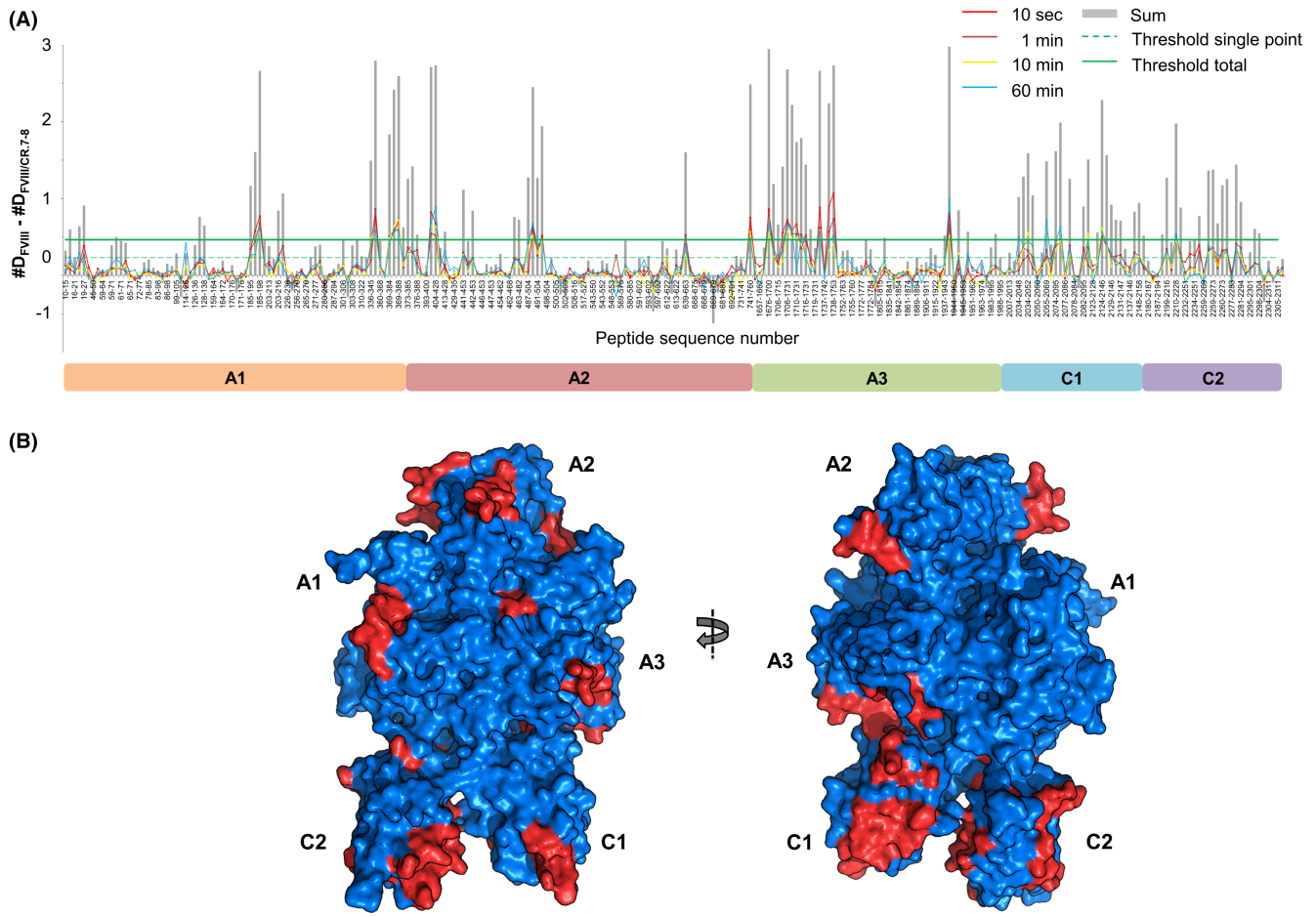


**FIGURE 6** Hydrogen–deuterium exchange mass spectrometry of factor VIII (FVIII) and CR.7–8 complex. A, Sequence coverage and difference plot (Δ#D) of peptide fragments of the B domain-deleted FVIII. Δ#D is FVIII minus FVIII/CR.7–8 for each identified peptide per deuterium incubation time point (color coded according to legend). The vertical gray bars are the sum of the Δ#D at each time point for a particular peptide. Horizontal green lines are 98% confidence intervals (CI): solid line for the sum of Δ#D, and dashed line for individual time point Δ#D. Two criteria used to determine a statistically significant difference in deuterium for a particular peptide: (i) at least two individual time points display Δ#D(t) > 98% CI (inner dashed), and (ii) sum of all Δ#D(t) > 98% CI (outer solid line). B, Surface plot of FVIII incubated with CR.7–8 based on the crystal structure of FVIII (PDB ID 6MF2). Peptides displayed no changes and regions not covered by peptide following complex formation with CR.7–8 are colored in blue, and peptides met the two criteria are colored in red.

motions, either cluster II or IV can interact with a large surface on FVIII encompassing the A3, C1, C2 domains, and beyond (>150 Å across the molecule).

This model considers the previously suggested model of RAP–LRP1 interaction exclusively dependent on switching canonical bivalent contacts[45] and several models of FVIII–LRP1 interaction based on involvement of: (i) several adjacent CR domains,[50,57] (ii) alternative CR doublets,[51] and (iii) cluster II with multiple FVIII lysine residues, where the interaction starts from the bottom of the C1 domain and extends to the top of the A3 domain.[47] Notably, this mode is intermedial between two well-known modes of biomolecular interactions based on: (i) reestablishing of *the same* contacts (majority of interactions) and (ii) consequent formation of *new* contacts upon unidirectional moving of one molecule along another (reactions of gene expression, etc.).

The proposed model may be relevant to other interactions of the LDLR family allowing for a deeper insight on why CRs are organized in clusters. Indeed, a flexible string of CR domains bearing sites with strong negative charge has high capacity to adapt multiple ligands via positively charged determinants. In this process, closed positioning of adjacent CR domains providing the bivalent canonical interaction significantly increases its specificity and strength compared to the monovalent interaction of a single CR. Apparent simplicity and universality of this mechanism may be related to the appearance of the LDLR family at an early stage of evolution as appearance of multicellular organisms.[23]

We believe that our findings will facilitate understanding of other LDLR family interactions associated with pathogenesis[27,28,30,31] and improving respective therapeutics and disease treatments. Regarding hemophilia A, our results suggest that development of a longer-acting therapeutical FVIII may be based on shielding of its large LRP1-binding site via a fusion of a thrombin-cleavable protein, allowing FVIII activation during blood coagulation. Similar design concept resulted in significant prolongation of the FVIII therapeutic effect in a recent clinical trial.[69]

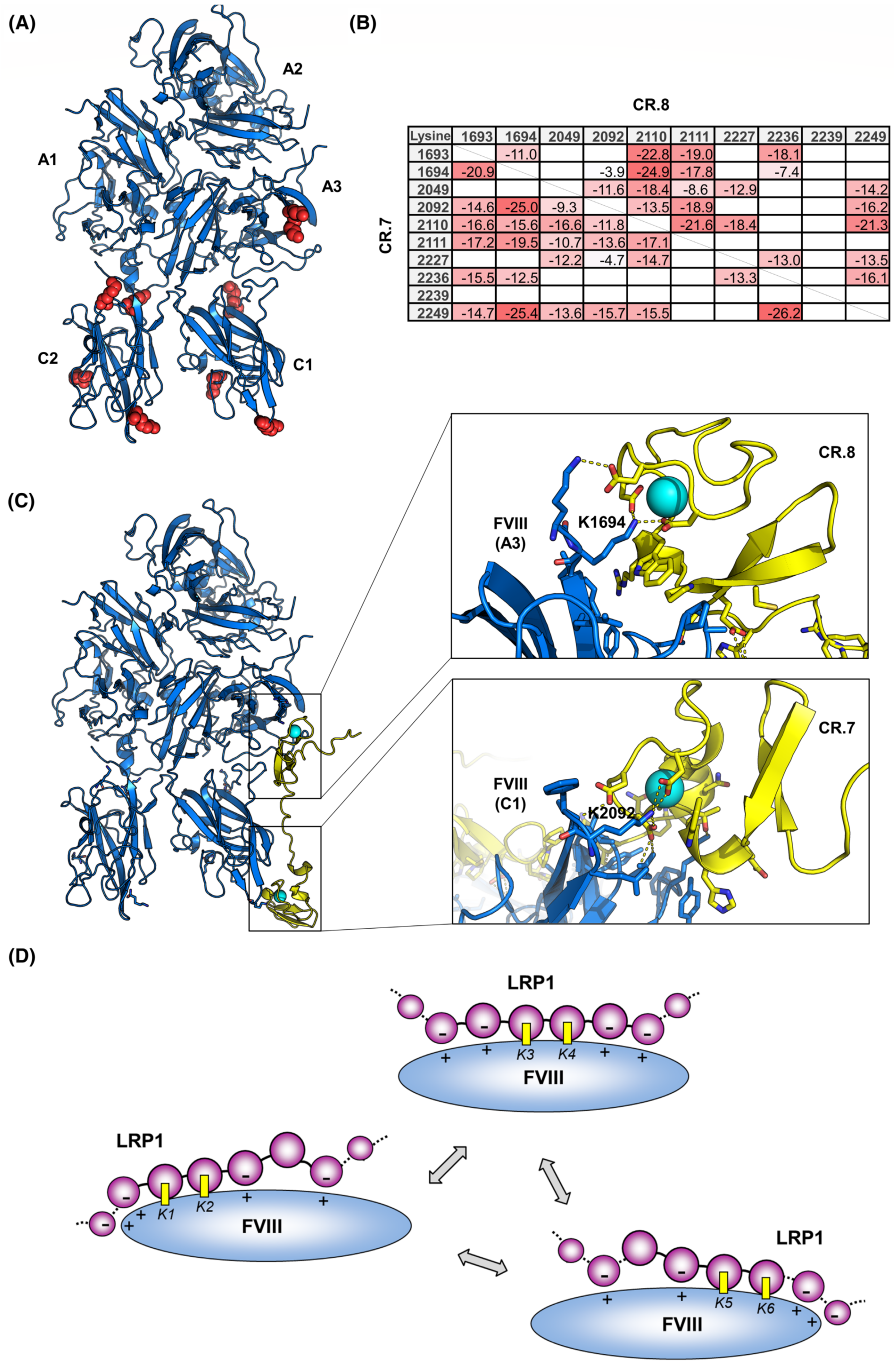


**FIGURE 7** Models of factor VIII (FVIII)-CR.7–8 and FVIII-lipoprotein receptor-related protein 1 (LRP1) complexes. A, FVIII structure (PDB ID 6MF2) showing 10 lysine residues (red) on the A3, C1, and C2 domains (LCh) within regions identified by hydrogen–deuterium exchange mass spectrometry as possibly contacting with CR.7–8. B, Binding energy profile for the docking combinations of CR.7–8 and the 10 lysine residues on the LCh. Unit of ΔΔG values is based on Rosetta energy unit (REU). C, A particular docking combination between FVIII (blue) and CR.7–8 (yellow). The canonical interactions between K2092 and K1694 of FVIII showing the "acidic pockets" and conserved W1032 on CR.7 and W1080 on CR.8 are enlarged in the box. Calcium ions coordinated by each complement-type repeat (CR) are shown as cyan-colored spheres. The protein structure images were generated using PyMOL 2.5.2 program (Schrödinger). D, A proposed model of FVIII interaction with LRP1. Initial recognition of FVIII is provided by either CR cluster II or IV (purple) via weak non-canonical multiple interactions of negatively charged residues (aspartic acid and glutamic acid) within CR domains with positively charged residues (lysine and arginine) on FVIII (blue). This facilitates interaction of a CR doublet of the cluster with a pair of "critical" lysine residues of FVIII ($K_x$ and $K_{x+1}$, yellow) on the C1 domain or surrounding area via the canonical (bivalent) binding providing a dominant binding energy. Over time, these binding combinations are switched to alternative CR domains of the cluster and other positively charged residues on FVIII. The resulting complex is formed by alternative binding combinations involving the canonical bivalent and non-canonical electrostatic interactions in dynamic equilibrium. Hence, the interactive region on FVIII represents the totality of its determinants involved in all binding combinations.

## AUTHOR CONTRIBUTIONS

H.C. performed experiments, analyzed results, and wrote the manuscript. Experimental data were also generated by J.H.K., S.A.S., P.O. (also contributed to manuscript editing), E.M., G.U.H., E.K., M.M., J.O., A.K.S., P.L.W., P.D., K.P., D.D., and D.K.S. (also provided helpful discussions and contributed to manuscript editing). A.G.S. designed the study, analyzed and interpreted results, and wrote the manuscript. All authors read and participated in editing of the final version of manuscript.

## ACKNOWLEDGMENTS

This work was supported by funds from the U.S. FDA/CBER project 05010 (AGS), R35 HL135743 (DKS), and the Ministry of Oceans and Fisheries, Korea 20210647 (KP). This work was also supported by U.S. FDA/CBER, appointments to the research program administered by the Oak Ridge Institute for Science and Education through an interagency agreement with the U.S. Department of Energy, and by the University of Maryland Baltimore, School of Pharmacy Mass Spectrometry Center (SOP1841-IQB2014). The authors are thankful to Novo Nordisk Inc. for providing high-quality FVIII (B domain-truncated) used in HDX-MS experiment, Dr. Marianne Kjalke and Dr. Johan Faber for support with this experiment, Dr. Koen Mertens for discussion of the mechanism of FVIII–LRP1 interaction, and Dr. Alexey Khrenov for helpful critique of the manuscript draft.

## CONFLICTS OF INTEREST

The authors declare that they have no conflicts of interests with the contents of this article. These contributions are an informal communication and represent the best judgment of the authors, and do not bind or obligate the U.S. FDA, and do not represent the official views of the National Institutes of Health. Mentioning specific products was not intended to point out any advantage or disadvantage of one product over others and was solely due to research purpose.

## ORCID

*Haarin Chun* https://orcid.org/0000-0002-2668-6296
*James H. Kurasawa* https://orcid.org/0000-0001-7869-0396
*Philip Olivares* https://orcid.org/0000-0003-3182-5884
*Ekaterina S. Marakasova* https://orcid.org/0000-0002-6505-4726
*Svetlana A. Shestopal* https://orcid.org/0000-0003-0725-5885
*Gabriela U. Hassink* https://orcid.org/0000-0002-2035-4848
*Elena Karnaukhova* https://orcid.org/0000-0002-8056-4812
*Mary Migliorini* https://orcid.org/0000-0001-9167-7444
*Juliet O. Obi* https://orcid.org/0000-0002-6851-0096
*Ally K. Smith* https://orcid.org/0000-0003-4539-1714
*Patrick L. Wintrode* https://orcid.org/0000-0003-1866-9397
*Prasannavenkatesh Durai* https://orcid.org/0000-0002-1538-8349
*Keunwan Park* https://orcid.org/0000-0002-8783-9495
*Daniel Deredge* https://orcid.org/0000-0002-6897-6523
*Dudley K. Strickland* https://orcid.org/0000-0001-7526-5917
*Andrey G. Sarafanov* https://orcid.org/0000-0001-6124-9713

## REFERENCES

1. Schwarz HP, Lenting PJ, Binder B, et al. Involvement of low-density lipoprotein receptor-related protein (LRP) in the clearance of factor VIII in von Willebrand factor-deficient mice. *Blood*. 2000;95:1703-1708.
2. Terraube V, O'Donnell JS, Jenkins PV. Factor VIII and von Willebrand factor interaction: biological, clinical and therapeutic importance. *Haemophilia*. 2010;16:3-13.
3. Fay PJ, Haidaris PJ, Smudzin TM. Human factor VIIIa subunit structure. Reconstruction of factor VIIIa from the isolated A1/A3-C1-C2 dimer and A2 subunit. *J Biol Chem*. 1991;266:8957-8962.
4. Mannucci PM, Cortesi PA, Di Minno MND, Sano M, Mantovani LG, Di Minno G. Comparative analysis of the pivotal studies of extended half-life recombinant FVIII products for treatment of haemophilia A. *Haemophilia*. 2021;27:e422-e433.
5. Bovenschen N, Mertens K, Hu L, Havekes LM, van Vlijmen BJ. LDL receptor cooperates with LDL receptor-related protein in regulating plasma levels of coagulation factor VIII in vivo. *Blood*. 2005;106:906-912.
6. Bovenschen N, Rijken DC, Havekes LM, van Vlijmen BJ, Mertens K. The B domain of coagulation factor VIII interacts with the asialoglycoprotein receptor. *J Thromb Haemost*. 2005;3:1257-1265.
7. Lenting PJ, Neels JG, van Den Berg BM, et al. The light chain of factor VIII comprises a binding site for low density lipoprotein receptor-related protein. *J Biol Chem*. 1999;274:23734-23739.
8. Pegon JN, Kurdi M, Casari C, et al. Factor VIII and von Willebrand factor are ligands for the carbohydrate-receptor Siglec-5. *Haematologica*. 2012;97:1855.
9. Saenko EL, Yakhyaev AV, Mikhailenko I, Strickland DK, Sarafanov AG. Role of the low density lipoprotein-related protein receptor in mediation of factor VIII catabolism. *J Biol Chem*. 1999;274:37685-37692.
10. Swystun LL, Lai JD, Notley C, et al. The endothelial cell receptor stabilin-2 regulates VWF-FVIII complex half-life and immunogenicity. *J Clin Invest*. 2018;128:4057-4073.
11. Swystun LL, Notley C, Georgescu I, et al. The endothelial lectin clearance receptor CLEC4M binds and internalizes factor VIII in a VWF-dependent and independent manner. *J Thromb Haemost*. 2019;17:681-694.
12. Swystun LL, Ogiwara K, Lai JD, et al. The scavenger receptor SCARA5 is an endocytic receptor for von Willebrand factor expressed by littoral cells in the human spleen. *J Thromb Haemost*. 2019;17:1384-1396.
13. Ward SE, O'Sullivan JM, Drakeford C, et al. A novel role for the macrophage galactose-type lectin receptor in mediating von Willebrand factor clearance. *Blood*. 2018;131:911-916.
14. Wohner N, Muczynski V, Mohamadi A, et al. Macrophage scavenger-receptor SR-AI contributes to the clearance of von Willebrand factor. *Haematologica*. 2018;103:728-737.
15. Bovenschen N, Herz J, Grimbergen JM, et al. Elevated plasma factor VIII in a mouse model of low-density lipoprotein receptor-related protein deficiency. *Blood*. 2003;101:3933-3939.
16. Brown MS, Herz J, Goldstein JL. LDL-receptor structure. Calcium cages, acid baths and recycling receptors. *Nature*. 1997;388:629-630.
17. Lee BY, Chon J, Kim HS, et al. Association between a polymorphism in CASP3 and CASP9 genes and ischemic stroke. *Ann Rehabil Med*. 2017;41:197-203.
18. Vormittag R, Bencur P, Ay C, et al. Low-density lipoprotein receptor-related protein 1 polymorphism 663 C > T affects clotting factor VIII activity and increases the risk of venous thromboembolism. *J Thromb Haemost*. 2007;5:497-502.
19. Paciullo F, Petito E, Falcinelli E, Gresele P, Momi S. Pleiotropic effects of PCSK9-inhibition on hemostasis: anti-PCSK9 reduce FVIII levels by enhancing LRP1 expression. *Thromb Res*. 2022;213:170-172.

20. Castro-Nunez L, Koornneef JM, Rondaij MG, et al. Cellular uptake of coagulation factor VIII: elusive role of the membrane-binding spikes in the C1 domain. *Int J Biochem Cell Biol*. 2017;89:34-41.
21. Sarafanov AG, Ananyeva NM, Shima M, Saenko EL. Cell surface heparan sulfate proteoglycans participate in factor VIII catabolism mediated by low density lipoprotein receptor-related protein. *J Biol Chem*. 2001;276:11970-11979.
22. Butenas S, Parhami-Seren B, Undas A, Fass DN, Mann KG. The "normal" factor VIII concentration in plasma. *Thromb Res*. 2010;126:119-123.
23. Dieckmann M, Dietrich MF, Herz J. Lipoprotein receptors--an evolutionarily ancient multifunctional receptor family. *Biol Chem*. 2010;391:1341-1363.
24. Lillis AP, Van Duyn LB, Murphy-Ullrich JE, Strickland DK. LDL receptor-related protein 1: unique tissue-specific functions revealed by selective gene knockout studies. *Physiol Rev*. 2008;88:887-918.
25. Gent J, Braakman I. Low-density lipoprotein receptor structure and folding. *Cell Mol Life Sci*. 2004;61:2461-2470.
26. Krieger M, Herz J. Structures and functions of multiligand lipoprotein receptors: macrophage scavenger receptors and LDL receptor-related protein (LRP). *Annu Rev Biochem*. 1994;63:601-637.
27. Au DT, Strickland DK, Muratoglu SC. The LDL receptor-related protein 1: at the crossroads of lipoprotein metabolism and insulin signaling. *J Diabetes Res*. 2017;2017:8356537.
28. Cooper JM, Lathuiliere A, Migliorini M, et al. Regulation of tau internalization, degradation, and seeding by LRP1 reveals multiple pathways for tau catabolism. *J Biol Chem*. 2021;296:100715.
29. Dlugosz P, Nimpf J. The reelin receptors apolipoprotein E receptor 2 (ApoER2) and VLDL receptor. *Int J Mol Sci*. 2018;19:3090.
30. Go GW, Mani A. Low-density lipoprotein receptor (LDLR) family orchestrates cholesterol homeostasis. *Yale J Biol Med*. 2012;85:19-28.
31. Lane-Donovan C, Philips GT, Herz J. More than cholesterol transporters: lipoprotein receptors in CNS function and neurodegeneration. *Neuron*. 2014;83:771-787.
32. Ananyeva NM, Makogonenko YM, Kouiavskaia DV, et al. The binding sites for the very low density lipoprotein receptor and low-density lipoprotein receptor-related protein are shared within coagulation factor VIII. *Blood Coagul Fibrinolysis*. 2008;19:166-177.
33. Ananyeva NM, Makogonenko YM, Sarafanov AG, et al. Interaction of coagulation factor VIII with members of the low-density lipoprotein receptor family follows common mechanism and involves consensus residues within the A2 binding site 484-509. *Blood Coagul Fibrinolysis*. 2008;19:543-555.
34. Mikhailenko I, Battey FD, Migliorini M, et al. Recognition of alpha 2-macroglobulin by the low density lipoprotein receptor-related protein requires the cooperation of two ligand binding cluster regions. *J Biol Chem*. 2001;276:39484-39491.
35. Actis Dato V, Chiabrando GA. The role of low-density lipoprotein receptor-related protein 1 in lipid metabolism, glucose homeostasis and inflammation. *Int J Mol Sci*. 2018;19:1780.
36. Fass D, Blacklow S, Kim PS, Berger JM. Molecular basis of familial hypercholesterolaemia from structure of LDL receptor module. *Nature*. 1997;388:691-693.
37. Guo Y, Yu X, Rihani K, Wang QY, Rong L. The role of a conserved acidic residue in calcium-dependent protein folding for a low density lipoprotein (LDL)-a module: implications in structure and function for the LDL receptor superfamily. *J Biol Chem*. 2004;279:16629-16637.
38. Fisher C, Beglova N, Blacklow SC. Structure of an LDLR-RAP complex reveals a general mode for ligand recognition by lipoprotein receptors. *Mol Cell*. 2006;22:277-283.
39. Verdaguer N, Fita I, Reithmayer M, Moser R, Blaas D. X-ray structure of a minor group human rhinovirus bound to a fragment of its cellular receptor protein. *Nat Struct Mol Biol*. 2004;11:429-434.
40. Yasui N, Nogi T, Takagi J. Structural basis for specific recognition of reelin by its receptors. *Structure*. 2010;18:320-331.
41. Bu G, Rennke S. Receptor-associated protein is a folding chaperone for low density lipoprotein receptor-related protein. *J Biol Chem*. 1996;271:22218-22224.
42. Herz J, Goldstein JL, Strickland DK, Ho YK, Brown MS. 39-kDa protein modulates binding of ligands to low density lipoprotein receptor-related protein/alpha 2-macroglobulin receptor. *J Biol Chem*. 1991;266:21232-21238.
43. Sato A, Shimada Y, Herz J, Yamamoto T, Jingami H. 39-kDa receptor-associated protein (RAP) facilitates secretion and ligand binding of extracellular region of very-low-density-lipoprotein receptor: implications for a distinct pathway from low-density-lipoprotein receptor. *Biochem J*. 1999;341:377-383.
44. Andersen OM, Christensen LL, Christensen PA, et al. Identification of the minimal functional unit in the low density lipoprotein receptor-related protein for binding the receptor- associated protein (RAP). A conserved acidic residue in the complement- type repeats is important for recognition of RAP. *J Biol Chem*. 2000;275:21017-21024.
45. Marakasova E, Olivares P, Karnaukhova E, et al. Molecular chaperone RAP interacts with LRP1 in a dynamic bivalent mode and enhances folding of ligand-binding regions of other LDLR family receptors. *J Biol Chem*. 2021;297:100842.
46. Young PA, Migliorini M, Strickland DK. Evidence that factor VIII forms a bivalent complex with the low density lipoprotein (LDL) receptor-related protein 1 (LRP1): identification of cluster IV on LRP1 as the major binding site. *J Biol Chem*. 2016;291:26035-26044.
47. van den Biggelaar M, Madsen JJ, Faber JH, et al. Factor VIII interacts with the endocytic receptor low-density lipoprotein receptor-related protein 1 via an extended surface comprising "hot-spot" lysine residues. *J Biol Chem*. 2015;290:16463-16476.
48. Neels JG, van Den Berg BM, Lookene A, Olivecrona G, Pannekoek H, van Zonneveld AJ. The second and fourth cluster of class a cysteine-rich repeats of the low density lipoprotein receptor-related protein share ligand-binding properties. *J Biol Chem*. 1999;274:31305-31311.
49. Bovenschen N, Boertjes RC, van Stempvoort G, et al. Low density lipoprotein receptor-related protein and factor IXa share structural requirements for binding to the A3 domain of coagulation factor VIII. *J Biol Chem*. 2003;278:9370-9377.
50. Meijer AB, Rohlena J, Van der ZC, et al. Functional duplication of ligand-binding domains within low-density lipoprotein receptor-related protein for interaction with receptor associated protein, alpha(2)-macroglobulin, factor IXa and factor VIII. *Biochim Biophys Acta*. 2007;1774:714-722.
51. Kurasawa JH, Shestopal SA, Woodle SA, Ovanesov MV, Lee TK, Sarafanov AG. Cluster III of low-density lipoprotein receptor-related protein 1 binds activated blood coagulation factor VIII. *Biochemistry*. 2015;54:481-489.
52. Thim L, Vandahl B, Karlsson J, et al. Purification and characterization of a new recombinant factor VIII (N8). *Haemophilia*. 2010;16:349-359.
53. Kurasawa JH, Shestopal SA, Jha NK, Ovanesov MV, Lee TK, Sarafanov AG. Insect cell-based expression and characterization of a single-chain variable antibody fragment directed against blood coagulation factor VIII. *Protein Expr Purif*. 2013;88:201-206.
54. Ashcom JD, Tiller SE, Dickerson K, Cravens JL, Argraves WS, Strickland DK. The human alpha 2-macroglobulin receptor: identification of a 420-kD cell surface glycoprotein specific for the activated conformation of alpha 2-macroglobulin. *J Cell Biol*. 1990;110:1041-1048.
55. Chun H, Catterton T, Kim H, Lee J, Kim BE. Organ-specific regulation of ATP7A abundance is coordinated with systemic copper homeostasis. *Sci Rep*. 2017;7:12001.
56. Chun H, Pettersson JR, Shestopal SA, et al. Characterization of protein unable to bind von Willebrand factor in recombinant factor VIII products. *J Thromb Haemost*. 2021;19:954-966.

57. Kurasawa JH, Shestopal SA, Karnaukhova E, Struble EB, Lee TK, Sarafanov AG. Mapping the binding region on the low density lipoprotein receptor for blood coagulation factor VIII. *J Biol Chem*. 2013;288:22033-22041.
58. Fields JK, Kihn K, Birkedal GS, et al. Molecular basis of selective cytokine signaling inhibition by antibodies targeting a shared receptor. *Front Immunol*. 2021;12:779100.
59. Sestok AE, Brown JB, Obi JO, et al. A fusion of the Bacteroides fragilis ferrous iron import proteins reveals a role for FeoA in stabilizing GTP-bound FeoB. *J Biol Chem*. 2022;298:101808.
60. Webb B, Sali A. Comparative protein structure modeling using MODELLER. *Curr Protoc Bioinformatics*. 2016;54:561-5637.
61. Tyka MD, Keedy DA, Andre I, et al. Alternate states of proteins revealed by detailed energy landscape mapping. *J Mol Biol*. 2011;405:607-618.
62. Bloem E, van den Biggelaar M, Wroblewska A, et al. Factor VIII C1 domain spikes 2092-2093 and 2158-2159 comprise regions that modulate cofactor function and cellular uptake. *J Biol Chem*. 2013;288:29670-29679.
63. Andersen OM, Petersen HH, Jacobsen C, et al. Analysis of a two-domain binding site for the urokinase-type plasminogen activator-plasminogen activator inhibitor-1 complex in low-density-lipoprotein-receptor-related protein. *Biochem J*. 2001;357:289-296.
64. Dolmer K, Campos A, Gettins PG. Quantitative dissection of the binding contributions of ligand lysines of the receptor-associated protein (RAP) to the low density lipoprotein receptor-related protein (LRP1). *J Biol Chem*. 2013;288:24081-24090.
65. Frostell A, Vinterback L, Sjobom H. Protein-ligand interactions using SPR systems. *Methods Mol Biol*. 2013;1008:139-165.
66. Migliorini M, Li SH, Zhou A, Emal CD, Lawrence DA, Strickland DK. High-affinity binding of plasminogen-activator inhibitor 1 complexes to LDL receptor-related protein 1 requires lysines 80, 88, and 207. *J Biol Chem*. 2020;295:212-222.
67. Prasad JM, Young PA, Strickland DK. High affinity binding of the receptor-associated protein D1D2 domains with the low density lipoprotein receptor-related protein (LRP1) involves bivalent complex formation: critical roles of Lysines 60 and 191. *J Biol Chem*. 2016;291:18430-18439.
68. van den Biggelaar M, Sellink E, Klein Gebbinck JW, Mertens K, Meijer AB. A single lysine of the two-lysine recognition motif of the D3 domain of receptor-associated protein is sufficient to mediate endocytosis by low-density lipoprotein receptor-related protein. *Int J Biochem Cell Biol*. 2011;43:431-440.
69. Konkle BA, Shapiro AD, Quon DV, et al. BIVV001 fusion protein as factor VIII replacement therapy for hemophilia a. *N Engl J Med*. 2020;383:1018-1027.

## SUPPORTING INFORMATION

Additional supporting information can be found online in the Supporting Information section at the end of this article.

**How to cite this article:** Chun H, Kurasawa JH, Olivares P, et al. Characterization of interaction between blood coagulation factor VIII and LRP1 suggests dynamic binding by alternating complex contacts. *J Thromb Haemost*. 2022;20:2255-2269. doi: 10.1111/jth.15817